Energy-Aware Dynamic Mission Planning Algorithm for UAVs

Adam Seewald[1], Hector Garcia de Marina[2], and Ulrik Pagh Schultz[1]

Abstract— abstract abstract abstract abstract abstract abstract abstract abstract abstract abstract abstract abstract abstract abstract abstract

I. INTRODUCTION

Planning a mission for unmanned aerial vehicles (UAVs) operating outdoors is a challenging task. Scenarios such as precision agriculture, search and rescue, and surveillance require advanced levels of autonomy along with strictly limited energy budgets–with the typical instance being a UAV used to inform its grounded counterparts of patterns detected while flying. Currently, UAVs flying outdoors are often semi-autonomous, in the sense that the mission is static and usually defined using a mission planning software [1]. Such a state of practice has prompted us to propose an *energy-aware dynamic mission planning algorithm* for UAVs. The algorithm attempts to combine and generalize some of the past body of knowledge on the mobile robot planning problem, and highlights the increasing *computational demands* and their relation to energy consumption, path, and autonomy.

Planning algorithms for mobile robots broadly are not a new concept, in that they are correlated to such topics as trajectory generation and path planning. Generally, these algorithms select an energy-optimized trajectory [2], by e.g., maximizing the operational time [3], but in practice apply to few robots [4], and focus on optimizing motion control for these robots [5], despite compelling evidence for the systems' energy being influenced by the computations over bare motion [6]. For UAVs specifically, rotorcrafts have equally gained research interest in terms of algorithms for energy-optimized trajectory generation [7], [8]. Furthermore, past mission planning algorithms–which include a broader

concept of a mission being a set of tasks along with a motion plan–also focus on the trajectory [6], [9], and apply to few robots [10], [11]. Yet, computations of such systems are only expected to increase in the near future.

The proposed algorithm alters the energy consumption dynamically by means of mission-specific parameters: the Quality of Service (QoS) of the computations, and the trajectory-explicit equations (TEEs) adjustments. In the remainder of the paper, we strictly adopt the following notation. We refer to the values of mission-specific QoS and TEEs parameters as computations and adjustments, to the constraints sets that delimit such computations and adjustments as QoS and TEEs sets, and to the current trajectory as TEE. Our goal is a mission extension by optimizing both computations and adjustments as the UAV flies and its batteries drain. First, the algorithm optimizes computations requiring the UAV to include robot operating system (ROS) nodes. Then, it optimizes adjustments–a way to alter the trajectory–and guides the UAV using a vector field [12] that converges smoothly to such trajectory. It relies on the assumptions of the mission being *periodic* and *uncertain*. The periodicity is directly observed, by e.g., the UAV flying in repetitive patterns, and the uncertainty accounts for the environmental interference with e.g., a fixed-wing UAV drifting due to windy weather. It addresses the periodicity modeling the energy with Fourier analysis–being the mission periodic, we expect the energy to evolve also periodically–and the uncertainty with a state estimator. It output the controls sequence (computations and adjustments) using robust output feedback model predictive control (MPC).

In the spirit of reducing costs, and resources, we showcase the algorithm using the problem of dynamic mission planning for a precision agriculture fixed-wing UAV. Such a scenario is often put into practice [13] with ground mobile robots used for harvesting [14]–[19], and UAVs for preventing damage and ensuring better crop quality [1], [20]. The mission consists of a UAV flying in circles and lines covering a polygon, detecting obstacles using a convolutional neural network (CNN), and informing grounded mobile robots employed for future harvesting–a survey mission optimized for the craft's dynamics. The algorithm plans the mission controlling the processing rate and the radius of the circles, affecting the distance between the lines. Data indicates a potential extension of up to 13 minutes over an hour by merely switching to the lowest computations. Figure 1 shows an initial slice of such a mission. The UAV first heads to the circular TEE φ_0, and later shifts to TEE φ_0^+, as e.g., windy weather required the adjustment of the control sequence to avoid battery depletion.

The remainder of the paper is organized as follows. The overview of dynamic mission planning is set in Section II, along with a suitable model for the position and energy. The algorithm that uses the model and solves the UAV dynamic mission planning problem is proposed in Section III. Section IV presents the result and showcase the performances. The paper finishes with some conclusions in Section V.

II. MISSION PLANNING OVERVIEW

Let a mission's stage be a generic continuous twice differentiable TEE φ and a set of tasks $\psi_1, \ldots, \psi_\sigma$. Moreover, let t_f be the final time, $[\cdot]$ the set $\{0, 1, \ldots, \cdot\}$, $[\cdot]^+$ the set $\{0\}/[\cdot]$, and $\underline{\cdot}, \overline{\cdot}$ the lower and upper bound of $\cdot$. If $\cdot$ is a value, the bounds are user defined and retrieved from a lookup table; if a set, they correspond to minimum and maximum of the set.

Definition II.1 (Stage and mission). At a time instant $k \in [0, t_f)$, the *stage* is defined as the ordered list

$$\mathcal{M}_k := \{(\varphi_k(\cdot), \psi_1(\cdot), \ldots, \psi_\sigma(\cdot)) \mid$$
$$\exists \, \varphi_k(\cdot) \in \mathbb{C}_k, \qquad (1)$$
$$\psi_i(\cdot) \in \mathbb{S}_{k,i} \, \forall i \in [\sigma]^+\},$$

where $\mathbb{C}_k := [\underline{c}_k, \overline{c}_k] \subseteq \mathbb{R}$ is the TEEs set, and $\mathbb{S}_{k,i} := [\underline{s}_{k,i}, \overline{s}_{k,i}] \subseteq \mathbb{Z}_{\geq 0}$ the i-th task QoS set. The parameters of the TEE φ_k are defined in Subsection II-A, of the tasks $\psi_1, \ldots, \psi_\sigma$ in II-C.

The *mission* is the union of all the stages, along with a function $\lambda : \mathbb{R}^2 \to \mathcal{M}_k$ which maps a point $\mathbf{p} \in \mathbb{R}^2$ of a UAV flying at an assigned altitude $h \in \mathbb{R}_{>0}$ w.r.t. some inertial navigation frame $\mathcal{O}_W$ to a specific stage. If for simplicity the system is sampled discrete-time

$$\mathcal{M} := (\lambda(\mathbf{p}), \bigcup_{i \in [t_f]} \mathcal{M}_i), \qquad (2)$$

the algorithm inputs $\mathcal{M}$, initial position, and energy coefficients guess, and outputs the position, the instantaneous energy consumption, and the controls sequence–an action performed evolving the mission state.

A. State: position and energy

The state is the UAV's position in space and the energy coefficients in time. Despite we show a linear relation between the instantaneous energy consumption and the energy coefficients (Theorem III.1), the two are different. We show after the main results how such approach indeed allowed us variability in terms of the systems behaving periodically, piece-wise periodically, or merely linearly with sporadic periodicity.

The set

$$\mathcal{P}_k := \{\mathbf{p}_k \mid \varphi_k(\mathbf{p}_k, c_{k,1}, \ldots, c_{k,\rho}) \in \mathbb{C}_k\}, \qquad (3)$$

delimits the area where the k-th TEE $\varphi_k : \mathbb{R}^2 \times \mathbb{R}^\rho \to \mathbb{R}$ is free to evolve using ρ adjustments $\mathbf{c}_k := c_{k,1}, \ldots, c_{k,\rho}$ (gray area in Figure 1), being the TEE satisfied for all the approaching points $\varphi_k \to \mathbb{C}_k$.
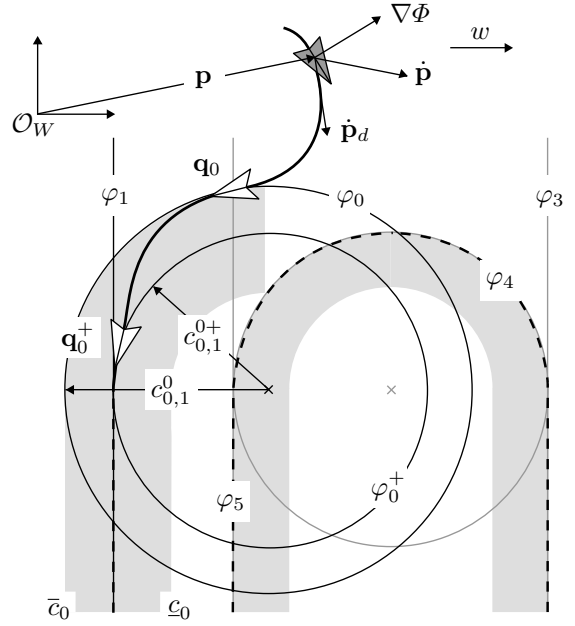

Fig. 1. The mission consists of circles and lines that forms a survey pattern. The UAV heads to φ_0 initially using the desired velocity vector $\dot{\mathbf{p}}_d$, but it later heads to φ_0^+ reducing the radius $c_{0,0}$ to satisfy the battery constraints (indeed the energy coefficients $\mathbf{q}_0$ evolution is higher then $\mathbf{q}_0^+$). The UAV then converges to φ_1, φ_2, φ_3, and so on until it covers the polygon (the circle φ_2 is not visible in the figure; it connects φ_1 and φ_3).

The algorithm uses the concept to select the adjustments s.t. $\varphi_k(\mathbf{p}_k, \mathbf{c}_k^0)$ has the highest energy value. It guides the UAV to the new position $\mathbf{p}_{k+1}$ using the vector field of $\Phi := \varphi_k(\mathbf{p}_k, \mathbf{c}_k^0)$, deriving the direction to follow–the desired velocity vector

$$\dot{\mathbf{p}}_d(\mathbf{p}_k) := E\nabla\Phi - k_e \Phi\nabla\Phi, \quad E = \begin{bmatrix} 0 & 1 \\ -1 & 0 \end{bmatrix}, \qquad (4)$$

where $\nabla\Phi \in \mathbb{R}^2$ is the gradient, E specifies the tracking direction, and $k_e \in \mathbb{R}_{\geq 0}$ the gain to adjusts the speed of convergence. The direction the velocity vector $\dot{\mathbf{p}}_d$ is pointing at is generally different from the course heading due to the atmospheric interference, such as wind $w \in \mathbb{R}$.

The algorithm models the energy using as state energy coefficients $\mathbf{q} \in \mathbb{R}^j$ derived from Fourier analysis (the meaning of j is clarified to the reader shortly) and decompose such evolution in the energy due to the trajectory, and computations–an approach adapted from our earlier work on computational energy analysis [21], [22], and energy estimation of a fixed-wing UAV [23].

B. Energy evolution due to trajectory

Let us consider a Fourier series $h : \mathbb{R}_{\geq 0} \to \mathbb{R}$ of an arbitrary order $r \in \mathbb{Z}_{\geq 0}$ for the purpose of energy consumption modeling of the mission

$$h(t) = \sum_{n=0}^{r} a_n \cos(nt/\xi) + b_n \sin(nt/\xi), \qquad (5)$$

where $\xi \in \mathbb{R}$ is the characteristic time, and $a_n, b_n \in \mathbb{R}$ the Fourier series coefficients.

Suppose uncertainty in the form of $\mathbf{w}_k \in \mathbb{R}^j, v_k \in \mathbb{R}$ accounting for the unknown state and output is absent. The non-linear model in Equation (5) can be expressed using an equivalent linear discrete time-invariant state-space model

$$\begin{cases} \mathbf{q}_{k+1} &= A\mathbf{q}_k + B\mathbf{u}_k + \mathbf{w}_k, \\ y_k &= C\mathbf{q}_k + v_k \end{cases}, \quad (6)$$

where $y_k \in \mathbb{R}_{\geq 0}$ is the instantaneous energy consumption. The state $\mathbf{q}$ mimics the original Fourier series coefficients

$$\mathbf{q}_k = \begin{bmatrix} \alpha_0 & \alpha_1 & \beta_1 & \cdots & \alpha_r & \beta_r \end{bmatrix}^T,$$

$$A = \begin{bmatrix} 1 & & & & \\ & A_1 & & & \\ & & \ddots & & \\ & & & A_r \end{bmatrix}, A_n = \begin{bmatrix} 0 & \frac{n}{\xi} \\ -\frac{n^2}{\xi^2} & 0 \end{bmatrix}, \quad (7)$$

$$C = \begin{bmatrix} 1 & 1 & 0 & \cdots & 1 & 0 \end{bmatrix},$$

where $\mathbf{q}_k \in \mathbb{R}^j$ given $j := 2r + 1$, $A \in \mathbb{R}^{j \times j}$ is the state transmission matrix, and $C \in \mathbb{R}^j$ is the output matrix. In matrix A, the first value is one, A_n is later on the diagonal, and zero in the remainder.

The control $\mathbf{u}$ along with the input matrix

$$\mathbf{u}_k = \begin{bmatrix} g(\mathbf{s}_k) - g(\mathbf{s}_{k-1}) & \mathbf{c}_k - \mathbf{c}_{k-1} \end{bmatrix}^T,$$

$$B = \begin{bmatrix} 1 & \omega_{k,1} & \cdots & \omega_{k,\rho} \\ & 0 & & \\ & & \ddots & \\ & & & 0 \end{bmatrix}, \quad (8)$$

where $\mathbf{s}_k, g(\cdot)$ are defined in Subsection II-C, $\mathbf{u}_k \in \mathbb{R}^l$ is the control given $l := 1 + \rho$, and $B \in \mathbb{R}^{j \times l}$. Moreover, the first item is one, while the others on the first row are gain factors $\omega_k \in \mathbb{R}$, quantifying the contribution of a given adjustment to the instantaneous energy consumption.

Note that the controls sequence $\mathbf{u}_k^a := (\mathbf{c}_k, \mathbf{s}_k)$–an output of the algorithm–differs from the nominal control in Equation (6) $\mathbf{u}_k(\mathbf{u}_k^a, \mathbf{u}_{k-1}^a)$.

The energy evolution analysis necessitates the following realistic assumption.

Assumption II.1 (Energy evelution periodicity). Given two time instants $k_1, k_2 \in [t_f]$ s.t. $k_1 > k_2$ and a constant value $n \in \mathbb{R}_{>0}$, there exist an arbitrary constant displacement $e \in \mathbb{R}$

$$|y_k - y_{k+n}| = e \quad \forall k \in [k_1, k_2]. \quad (9)$$

Physically, the time evolution of the instantaneous energy consumption is assumed periodic, in the sense that it presents repetitive patterns. We show in Section IV the assumption being eased in practice to a set $\mathbb{E} \subset \mathbb{R}$, or omitted under specific conditions.

Equation (8) accounts for the energy due to the computations. The energy due to the adjustments is merely a linear combination of the gain factor and the adjustment. Nevertheless, the change updates the path which will hence affect the reading from the sensors and adjust the energy coefficients. For instance, a decrement in the adjustment

radius of a circle when the TEE is a circle, adds a negative contribution, thus simulates the lowering of instantaneous energy consumption.

C. Energy evolution due to computations

The energy cost of the computations (set of tasks being executed on an embedded board on the UAV) is assessed using `powprofiler`, an open-source modeling tool presented in our previous work [21], that measures software configurations empirically and builds a computational energy consumption model. Specifically, the tool builds a linear interpolation, one per each task. It requires the user to implement the mission as a ROS system with one or more ROS nodes changing the computational load by node-specific ROS parameters. A way to simulate the change of the computations.

The plan $\mathcal{M}$ contains a set of ordered lists with σ tasks each (recall Definition II.1). These tasks are simulated by σ ROS nodes $\Psi(\mathbf{s}_k) := (\psi_1(s_{k,1}), \ldots, \psi_\sigma(s_{k,\sigma}))$, in fact they input the desired and output the actual computations

$$\mathbf{s}_k := \left\{ s_{k,1}, \ldots, s_{k,\sigma} \mid \psi_i(s_{k,i}) \in \mathbb{S}_k \, \forall i \in [\sigma]^+ \right\}, \quad (10)$$

where $s_{k,i} : \mathbb{Z}_{\geq 0} \to \mathbb{Z}_{\geq 0}$ returns the i-th computation, $\mathbf{s}_k \in \mathbb{S}_k \subseteq \mathbb{Z}_{\geq 0}^\sigma$ the set of σ computations at time k given $\mathbb{S}_k := \bigcup_{i \in [\sigma]^+} \mathbb{S}_{k,i}$.

Let us further define $g : \mathbb{Z}_{\geq 0} \times \mathbb{Z}_{\geq 0} \to \mathbb{R}_{\geq 0}$ as the instantaneous computational energy consumption value obtained interrogating `powprofiler`

$$y_k^s := g\left(\mathrm{QoS}_{k,1}, \ldots, \mathrm{QoS}_{k,\sigma} \right) = g(\mathbf{s}_k). \quad (11)$$

Moreover, $g(\{\emptyset\}) = 0$.

III. ALGORITHM

Given an initial stage $\mathcal{M}_0$ (TEE φ_0, tasks Ψ, computations $\mathbf{s}_0 \in \mathbb{S}_0$, and adaptations $\mathbf{c}_0 \in \mathbb{C}_0$), the main purpose of the algorithm is to output a set of control sequences $\mathbf{u}^a := \{\mathbf{u}_0^a, \mathbf{u}_1^a, \ldots\}$ in a valid mission.

Definition III.1 (Valid mission). A mission is valid if for every stage $\mathcal{M}_{k-1}$ in $k \in [t_f]^+$ there exist a control sequence $\mathbf{u}_k^a$ that produce the next stage $\mathcal{M}_k$

$$\mathbf{u}_k^a = \{ (\mathbf{c}_k, \mathbf{s}_k) \mid \exists \, \mathbf{c}_{k-1} \in \mathbb{C}_{k-1}, \mathbf{s}_{k-1} \in \mathbb{S}_{k-1} \text{ and}$$
$$(\varphi(\mathbf{p}_{k-1}, \mathbf{c}_{k-1}), \Psi(\mathbf{s}_{k-1})) \in \mathcal{M}_{k-1} \quad (12)$$
$$\implies (\varphi(\mathbf{p}_k, \mathbf{c}_k), \Psi(\mathbf{s}_k)) \in \mathcal{M}_k \}.$$

Let us proof that if the mission is valid, the instantaneous energy consumption can be modeled as linear combination of the state from the Equation (6) for all $k \in [t_f]$.

Theorem III.1 (Periodic energy model). Consider the mission from Definition II.1, the valid mission from III.1. Assume Assumption II.1 holds, the model of Equation (6) behaves ideally ($\mathbf{w} = \mathbf{0}, v = 0$), the initial energy co-efficients state $\mathbf{q}_0$ is y_0^m/j for the first coefficient where $y_0^m \in \mathbb{R}_{>0}$ is an initial measurement[1], $(1/2)y_0^m/j$ for all

---

[1] y_0^m can be the initial measurement or the measurement from a previous instance of the algorithm

the others, and the mission is valid. Then, the instantaneous energy consumption y_k is a linear combination of the state $\mathbf{q}_k$.

Proof. The proof is based on mathematical induction. Base case: we proof that $y_0 = y_0^m$. Recall the definition of the state in Equation (7). The output is $y_0 = \alpha_{0,0} + \alpha_{0,1} + \cdots + \alpha_{0,r} = y_0^m/j + (1/2)y_0^m/j + \cdots + (1/2)y_0^m/j = y_0^m$.

Induction step: by inspection of Equation (6), the output at instant k can be expressed $y_k = (\alpha_{0,0} + B\mathbf{u}_0 + \cdots + B\mathbf{u}_{k-1}) + p_1(k)\alpha_{0,1} + \cdots + p_r(k)\alpha_{0,r}$, where $\forall n \in \mathbb{Z}_{\geq 2}$

$$p_r(n) := \begin{cases} \prod_{i=1}^{n/2} r^3/\xi^3 & \text{for even } n \\ (r/\xi)\prod_{i=1}^{(n-1)/2} r^3/\xi^3 & \text{for odd } n \end{cases}. \quad (13)$$

Suppose k is even and the theorem holds up to k. Initial energy coefficients state $\mathbf{q}_0$ leads to $y_k = (y_0^m/j + B\mathbf{u}_0 + \cdots + B\mathbf{u}_{k-1}) + p_1(k)(1/2)y_0^m/j + \cdots + p_r(k)(1/2)y_0^m/j = y_k^m$.

We prove now that the instantaneous energy consumption at $k+1$ is still a linear combination of the state. We express the output in function of the previous state $y_{k+1} = (\alpha_{0,0} + B\mathbf{u}_0 + \cdots + B\mathbf{u}_k) + (1/\xi)\beta_{k,1} + \cdots + (r/\xi)\beta_{k,r}$. Notice that the coefficients α, β have an equivalent evolution (indeed this allows to simulate the periodicity) and $\beta_{k,r} = p_r(k)\beta_{0,r}$. Thus, the output can be expressed $y_{k+1} = (\alpha_{0,0} + B\mathbf{u}_0 + \cdots + B\mathbf{u}_k) + (1/\xi)p_1(k)\beta_{0,1} + \cdots + (r/\xi)p_r(k)\beta_{0,r}$. The expression is equivalent to $y_{k+1} = (\alpha_{0,0} + B\mathbf{u}_0 + \cdots + B\mathbf{u}_k) + p_r(k+1)\beta_{0,r} + \cdots + p_r(k+1)\beta_{0,r}$ using the definition of p_r in Equation (13). Again, the state $\mathbf{q}_0$ leads to $y_{k+1} = (\alpha_{0,0} + B\mathbf{u}_0 + \cdots + B\mathbf{u}_k) + p_r(k+1)(1/2)y_0^m + \cdots + p_r(k+1)(1/2)y_0^m = y_{k+1}^m$, alike the previous statement ($y_k^m = y_{k+1}^m$), but at instant $k+1$. The proof for odd k is equivalent. ∎

A. Output constraints set

We stated earlier the output y_k–the instantaneous energy consumption–evolves in $\mathbb{R}_{\geq 0}$. This is generally untrue. Physical UAVs are bounded by strict battery limitations.

Let us hence consider the state of charge (SoC) of such battery with a simplistic difference equation [23]

$$\text{SoC}_k = -\left(V - \sqrt{V^2 - 4R_r\tilde{V}y_kV^{-1}}\right)/2R_rQ_c, \quad (14)$$

where $V \in \mathbb{R}$ is the internal battery and $\tilde{V} \in \mathbb{R}$ the stabilized voltage, $R_r \in \mathbb{R}$ the resistance, and $Q_c \in \mathbb{R}$ the constant nominal capacity. We define the output constraints set

$$\mathbb{Y}_k := \{y_k \mid y_k \in [0, \text{SoC}_kQ_cV] \subseteq \mathbb{R}_{\geq 0}\}, \quad (15)$$

where $\overline{\mathbb{Y}}_k$ is the maximum discharge capacity by the internal battery voltage–the maximum instantaneous energy consumption.

B. Deployment algorithm

1: **procedure** STEP($\mathbf{q}_{k-1}$, $\mathbf{u}_{k-1}^a$, $\mathbf{u}_{k-2}^a$, P_{k-1})
2:     $\mathbf{u}_{k-1} \leftarrow \mathbf{u}_{k-1}(\overline{\mathbf{u}}_{k-1}^a, \mathbf{u}_{k-2}^a)$
3:     $\mathbf{u}_{k-1}^0 \leftarrow \arg\max_{\mathbf{u}} \sum_{i=k-1}^{k+N-2} l(\mathbf{q}_i, \mathbf{u}_i) + V_f(\mathbf{q}_{k+N-1})$
4:     $\hat{\mathbf{q}}_k^- \leftarrow A\hat{\mathbf{q}}_{k-1} + B\mathbf{u}_{k-1}^0$

5:     **if** $C\hat{\mathbf{q}}_k^- \notin \mathbb{Y}_k$ **then**
6:         $\mathbf{u}_{k-1}^a \leftarrow \mathbf{u}_{k-1}^a/\{\overline{\mathbf{u}}_{k-1}^a\}$
7:         **return** STEP($\mathbf{q}_{k-1}$, $\mathbf{u}_{k-1}^a$, $\mathbf{u}_{k-2}^a$, P_{k-1})
8:     **else**
9:         **if** $|y_k^m - C\hat{\mathbf{q}}_k^-| \leq \varepsilon$ **then**
10:           $\hat{\mathbf{q}}_k \leftarrow \hat{\mathbf{q}}_k^-$
11:           $P_k \leftarrow P_k^-$
12:         **else**
13:           $P_k^- \leftarrow AP_{k-1}A^T + Q$
14:           $K \leftarrow P_k^- C^T/(CP_k^- C^T + R)$
15:           $\hat{\mathbf{q}}_k \leftarrow \hat{\mathbf{q}}_k^- + K(y_k^m - C\hat{\mathbf{q}}_k^-)$
16:           $P_k \leftarrow (I + KC)P_k^-$
17:         **end if**
18:         $\mathbf{u}_k^a \leftarrow \mathbf{u}_{k-1}^a$
19:         **return** $(\hat{\mathbf{q}}_k, P_k, \mathbf{u}_k^a)$
20:     **end if**
21: **end procedure**

22: **procedure** EADMPA($\mathcal{M}$, $\mathbf{p}_0$, $\mathbf{q}_0$)
23:     $k \leftarrow 0$
24:     $\mathbf{u}_{k-1}^a \leftarrow \{\emptyset\}$
25:     $\mathbf{p}_k \leftarrow \mathbf{p}_0$
26:     $\mathbf{q}_k \leftarrow \mathbf{q}_0$
27:     **while** $k \leq t_f$ **do**
28:         $\mathbf{u}_k^a \leftarrow \{\mathbf{u}_k^a \mid (\varphi_k(\mathbf{p}_k, \mathbf{c}_k), \Psi(\mathbf{s_k})) \in \mathcal{M}_k \subseteq \mathcal{M}\}$
29:         $(\mathbf{q}_k, P_k, \mathbf{u}_k^a) \leftarrow$ STEP($\mathbf{q}_k$, $\mathbf{u}_k^a$, $\mathbf{u}_{k-1}^a$, P_k)
30:         $\mathbf{p}_k \leftarrow \mathbf{p}_k\dot{\mathbf{p}}_d(\mathbf{p}_k)/v$
31:         $\mathbf{u}_{k-1}^a \leftarrow \mathbf{u}_k^a$
32:         $k \leftarrow k + 1$
33:     **end while**
34: **end procedure**

Per each time step, the algorithm updates the state–the position at line 30 and the energy coefficients at line 29–and the control sequence. Note that the position can be computed directly from Equation (4). If the velocity is $v \in \mathbb{R}_{\geq 0}$, and the starting point $\mathbf{p}_0$, $\mathbf{p}_{k+1} = \mathbf{p}_k\dot{\mathbf{p}}_d(\mathbf{p}_k)/v$.

In detail, initial guess for $P_0 \in \mathbb{R}^{j \times j}$ is positive definite and derived empirically, for $\mathbf{q}_0$ an initial measurement is distributed to the coefficients (see Theorem III.1). Line 2 selects the maximum possible control from the current control sequence. Line 3 uses robust output feedback model predictive control (MPC) [24] to select the optimal control $\mathbf{u}^0$ for a given horizon $N \in \mathbb{Z}_{>0}$ from the cost function

$$\begin{aligned} l(\mathbf{q}_k, \mathbf{u}_k) &:= (1/2)(\mathbf{q}_k^T Q\mathbf{q}_k + \mathbf{u}_k^T R\mathbf{u}_k), \\ V_f(\mathbf{q}_k) &:= (1/2)(\mathbf{q}_k^T P_f\mathbf{q}_k), \end{aligned} \quad (16)$$

where matrices $Q \in \mathbb{R}^{j \times j}$, $R \in \mathbb{R}^{l \times l}$ are positive definite.

Follows a check if the mission can finish without the eventuality of battery discharge (output constraints satisfaction) at line 5, with the control sequence being eventually updated and the process reiterated at line 7.

Before the next step, state estimator–the discrete-time Kalman filter [25] at lines 13–16–predicts the state $\mathbf{q}$ if the modeled instantaneous energy consumption diverges from the sensor's value $y_k^m \in \mathbb{R}$ more than a given $\varepsilon \in \mathbb{R}_{\geq 0}$, or sensor measurements are unavailable ($y_k^m = 0$).

IV. Evaluation

*

V. Conclusion and Future Work

*

References

[1] P. Daponte, L. De Vito, L. Glielmo, L. Iannelli, D. Liuzza, F. Picariello, and G. Silano, "A review on the use of drones for precision agriculture," in *IOP Conference Series: Earth and Environmental Science*, vol. 275, no. 1. IOP Publishing, 2019, p. 012022.

[2] Y. Mei, Y.-H. Lu, Y. C. Hu, and C. G. Lee, "Energy-efficient motion planning for mobile robots," in *IEEE International Conference on Robotics and Automation, 2004. Proceedings. ICRA'04. 2004*, vol. 5. IEEE, 2004, pp. 4344–4349.

[3] M. Wahab, F. Rios-Gutierrez, and A. El Shahat, *Energy modeling of differential drive robots*. IEEE, 2015.

[4] C. H. Kim and B. K. Kim, "Energy-saving 3-step velocity control algorithm for battery-powered wheeled mobile robots," in *Proceedings of the 2005 IEEE international conference on robotics and automation*. IEEE, 2005, pp. 2375–2380.

[5] H. Kim and B.-K. Kim, "Minimum-energy translational trajectory planning for battery-powered three-wheeled omni-directional mobile robots," in *2008 10th International Conference on Control, Automation, Robotics and Vision*. IEEE, 2008, pp. 1730–1735.

[6] Y. Mei, Y.-H. Lu, Y. C. Hu, and C. G. Lee, "A case study of mobile robot's energy consumption and conservation techniques," in *ICAR'05. Proceedings., 12th International Conference on Advanced Robotics, 2005*. IEEE, 2005, pp. 492–497.

[7] F. Morbidi, R. Cano, and D. Lara, "Minimum-energy path generation for a quadrotor uav," in *2016 IEEE International Conference on Robotics and Automation (ICRA)*. IEEE, 2016, pp. 1492–1498.

[8] N. Kreciglowa, K. Karydis, and V. Kumar, "Energy efficiency of trajectory generation methods for stop-and-go aerial robot navigation," in *2017 International Conference on Unmanned Aircraft Systems (ICUAS)*. IEEE, 2017, pp. 656–662.

[9] Y. Mei, Y.-H. Lu, Y. C. Hu, and C. G. Lee, "Deployment of mobile robots with energy and timing constraints," *IEEE Transactions on robotics*, vol. 22, no. 3, pp. 507–522, 2006.

[10] A. Sadrpour, J. Jin, and A. G. Ulsoy, "Mission energy prediction for unmanned ground vehicles using real-time measurements and prior knowledge," *Journal of Field Robotics*, vol. 30, no. 3, pp. 399–414, 2013.

[11] ——, "Experimental validation of mission energy prediction model for unmanned ground vehicles," in *2013 American Control Conference*. IEEE, 2013, pp. 5960–5965.

[12] H. G. De Marina, Y. A. Kapitanyuk, M. Bronz, G. Hattenberger, and M. Cao, "Guidance algorithm for smooth trajectory tracking of a fixed wing uav flying in wind flows," in *2017 IEEE international conference on robotics and automation (ICRA)*. IEEE, 2017, pp. 5740–5745.

[13] S. S. H. Hajjaj and K. S. M. Sahari, "Review of research in the area of agriculture mobile robots," in *The 8th International Conference on Robotic, Vision, Signal Processing & Power Applications*. Springer, 2014, pp. 107–117.

[14] F. Qingchun, Z. Wengang, Q. Quan, J. Kai, and G. Rui, "Study on strawberry robotic harvesting system," in *2012 IEEE International Conference on Computer Science and Automation Engineering (CSAE)*, vol. 1. IEEE, 2012, pp. 320–324.

[15] F. Dong, W. Heinemann, and R. Kasper, "Development of a row guidance system for an autonomous robot for white asparagus harvesting," *Computers and Electronics in Agriculture*, vol. 79, no. 2, pp. 216–225, 2011.

[16] Z. De-An, L. Jidong, J. Wei, Z. Ying, and C. Yu, "Design and control of an apple harvesting robot," *Biosystems engineering*, vol. 110, no. 2, pp. 112–122, 2011.

[17] A. Aljanobi, S. Al-Hamed, and S. Al-Suhaibani, "A setup of mobile robotic unit for fruit harvesting," in *19th International Workshop on Robotics in Alpe-Adria-Danube Region (RAAD 2010)*. IEEE, 2010, pp. 105–108.

[18] Z. Li, J. Liu, P. Li, and W. Li, "Analysis of workspace and kinematics for a tomato harvesting robot," in *2008 International Conference on Intelligent Computation Technology and Automation (ICICTA)*, vol. 1. IEEE, 2008, pp. 823–827.

[19] Y. Edan, D. Rogozin, T. Flash, and G. E. Miles, "Robotic melon harvesting," *IEEE Transactions on Robotics and Automation*, vol. 16, no. 6, pp. 831–835, 2000.

[20] V. Puri, A. Nayyar, and L. Raja, "Agriculture drones: A modern breakthrough in precision agriculture," *Journal of Statistics and Management Systems*, vol. 20, no. 4, pp. 507–518, 2017.

[21] A. Seewald, U. P. Schultz, E. Ebeid, and H. S. Midtiby, "Coarse-grained computation-oriented energy modeling for heterogeneous parallel embedded systems," *International Journal of Parallel Programming*, pp. 1–22, 2019.

[22] A. Seewald, U. P. Schultz, J. Roeder, B. Rouxel, and C. Grelck, "Component-based computation-energy modeling for embedded systems," in *Proceedings Companion of the 2019 ACM SIGPLAN International Conference on Systems, Programming, Languages, and Applications: Software for Humanity*. ACM, 2019, pp. 5–6.

[23] A. Seewald, H. Garcia de Marina, H. S. Midtiby, and U. P. Schultz, "Mechanical and computational energy estimation of a fixed-wing drone," in *2020 4th IEEE International Conference on Robotic Computing (IRC)*. IEEE, 2020, p. to appear. [Online]. Available: https://adamseew.bitbucket.io/short/mechanical2020

[24] J. B. Rawlings, D. Q. Mayne, and M. Diehl, *Model predictive control: theory, computation, and design*. Nob Hill Publishing Madison, WI, 2017, vol. 2.

[25] D. Simon, *Optimal state estimation: Kalman, H infinity, and nonlinear approaches*. John Wiley & Sons, 2006.